

Atmospheric blocking characteristics in two storm-resolving GCMs

Edgar Dolores-Tesillos and Olivia Martius

Oeschger Center for Climate Change Research and Institute of Geography, University of Bern, Switzerland

edgar.dolores@unibe.ch

Background

Atmospheric blocking and their associated extreme weather challenge the current climate models. Two next generations of storm-resolving Earth-system Models (**nextGEMS**) try to reduce these biases by improving resolution. These changes lead to a better representation of mesoscale processes. Here, we evaluate how the large-scale flow can benefit from the higher grid-resolution. Recent studies have proved the relevance of the diabatic processes for the block formation and intensification. Ascending Warm conveyor belts (WCB) airstreams transport air masses with negative potential vorticity (PV) anomalies into the upper-level ridge associated with the block and contribute to its intensification [4,5,6].

Data and methods

Atmospheric blocking properties in the Northern Hemisphere are investigated using a 5-year data set of Geopotential Height (GH) from the **nextGEMS**:

-**ICON** outputs consist of dx=5 km, dt=30 minutes, deep convection=off.

-**IFS** outputs consist of dx=4.4 km and dx=28 km, dt=1 hourly data, deep convection=on.

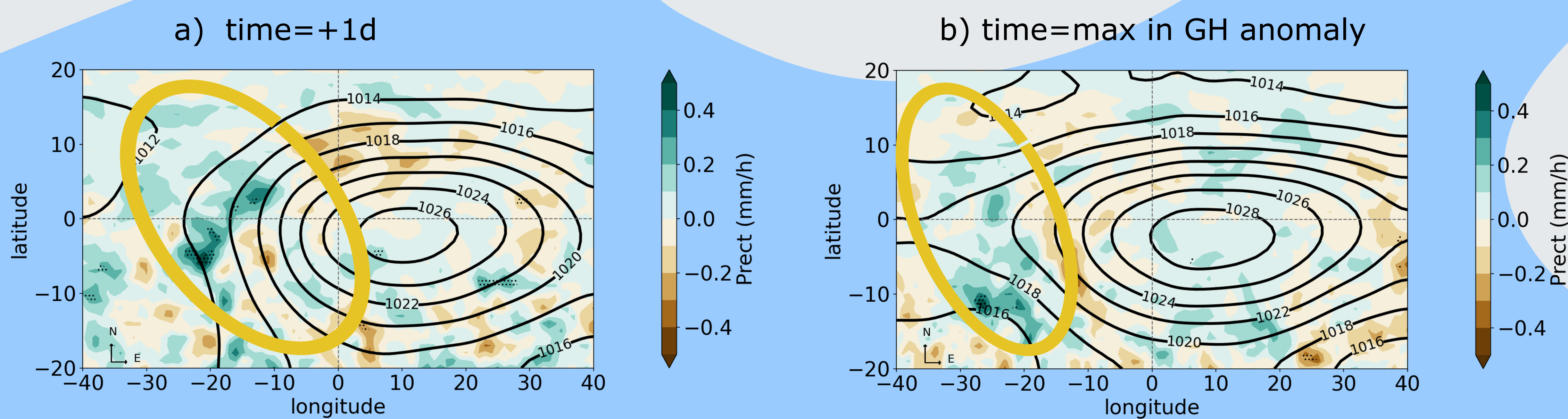
Reference: Reanalysis ERA5 (1990-2020) [1].

Comparison: one CMIP6 model (MPI-ESM1-2-LR), historical (1979-2014) [2].

Atmospheric blocking index:

Persistent and quasi-stationary mid-level (500 hPa) negative GH anomaly following the Schierz index [3].

Blocking-centered composites of precipitation difference between IFS-4.4 km and 28 km during blocking intensification



Increased upstream precipitation during blocking onset as the horizontal resolution increase help to produce stronger and larger atmospheric blockings

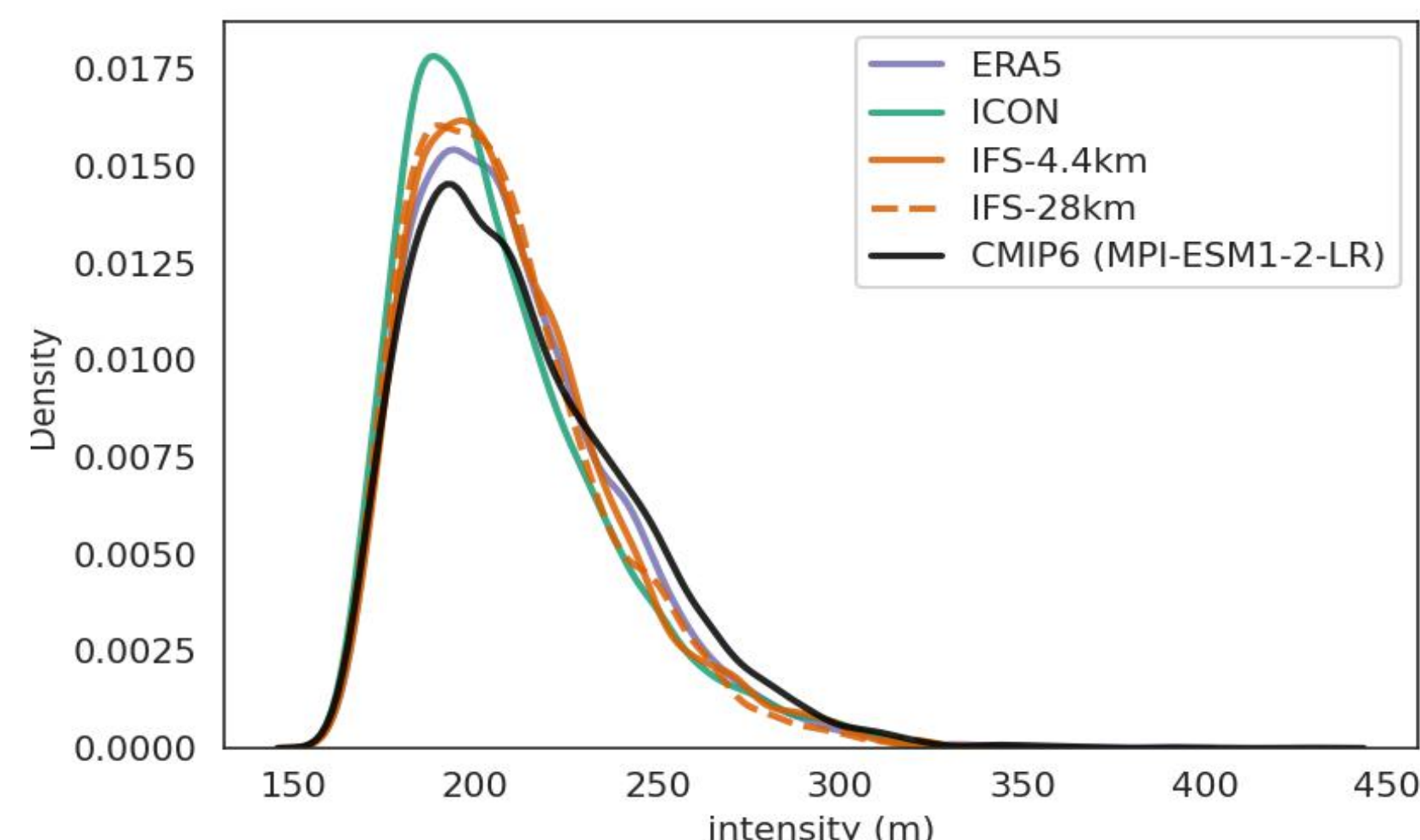
Figure 1. Precipitation difference between IFS at 4.4 km and 28 km (colors) and sea level pressure in IFS at 4.4 km (contours) at different times of lifecycle, a) one day and b) maximum intensity. Stippling indicates the grid points with significant differences based on the t-test with a significance level (p-value) of 0.05.

Key results

Individual blocks identified in ERA5(1990-2020) **ICON** **IFS-4.4 km** **IFS-28 km** CMIP6 (1979-2014):
39092 5648 5934 5472 43975

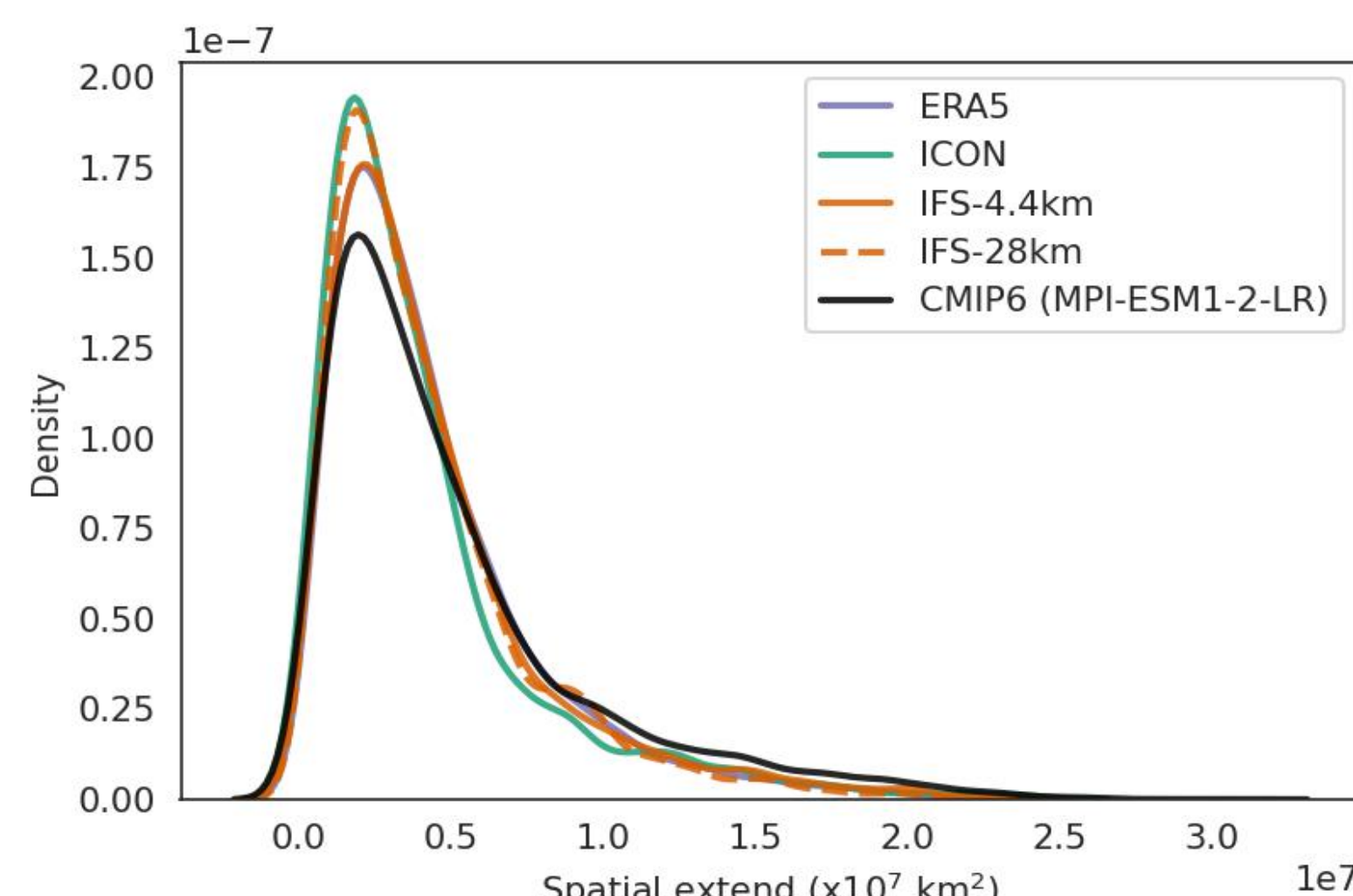
Density distribution functions show **nextGEMS** improvements in representing the atmospheric blocking intensity and size (Figs. 2 and 3). The median and the goodness of the fit test confirm quantitatively the higher skill, where the **IFS** seems to produce blockings more similar to ERA5 than the **ICON** model.

Figure 2. Intensity (m)



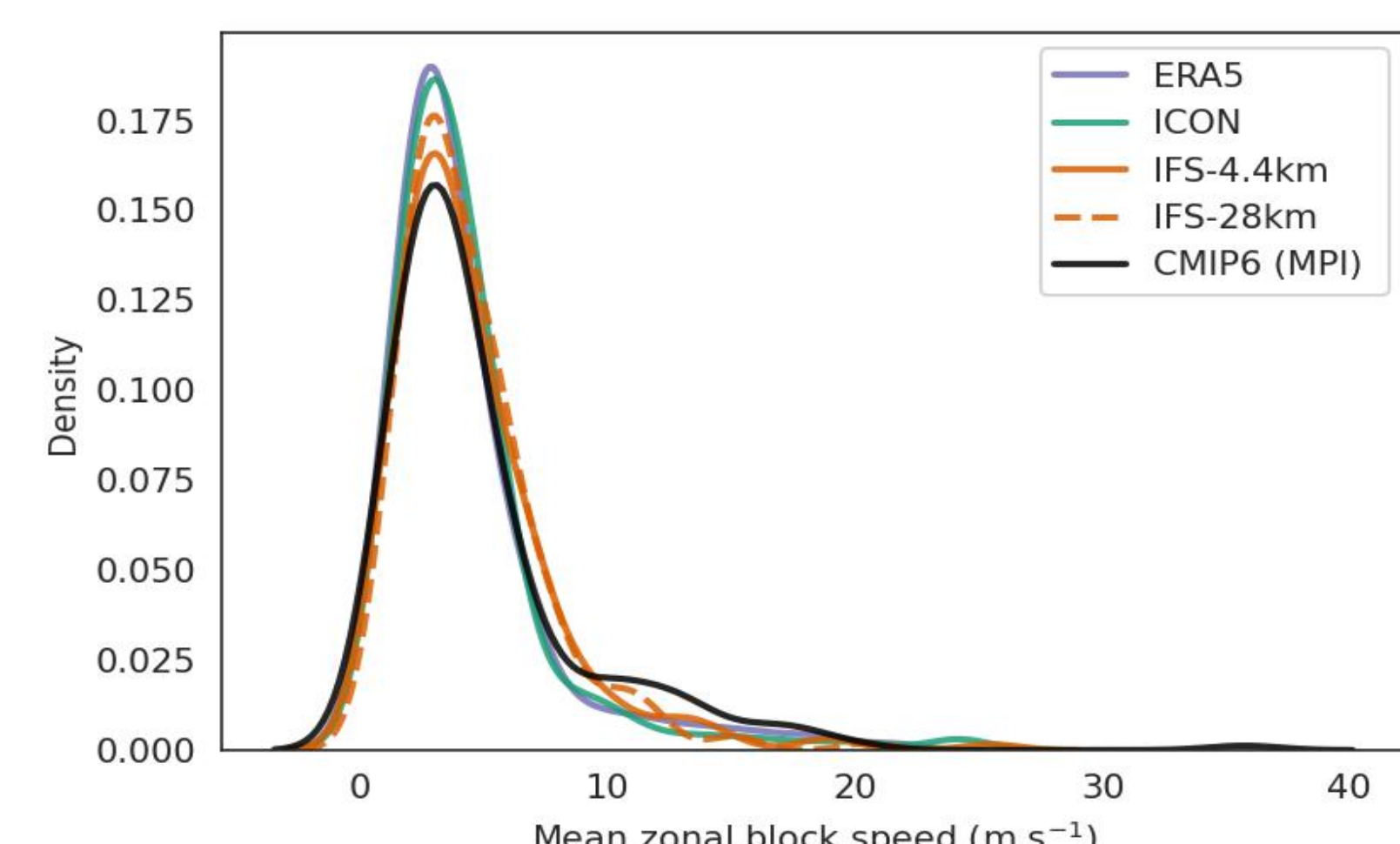
	Median (m)	Goodness of fit
ERA5	205.9	
ICON	200.8	30.1
IFS 4.4 KM	204.9	18.8
IFS 28 KM	203.7	25.0
CMIP6 (MPI)	207.8	36.9

Figure 3. Size (km²)



	Median (x10 ⁶ km ²)	Goodness of fit
ERA5	3.49	
ICON	3.04	31.0
IFS 4.4 KM	3.41	18.3
IFS 28 KM	3.26	25.2
CMIP6 (MPI)	3.66	34.4

Figure 4. Zonal speed (m/s)



	Median (m/s)	Goodness of fit
ERA5	3.22	
ICON	3.44	0.28
IFS 4.4 KM	3.54	0.25
IFS 28 KM	3.64	0.33
CMIP6 (MPI)	3.43	0.34

Take away

-**nextGEMS** captures the intensity and size of atmospheric blocking better than the chosen CMIP6 model, and the improvements are also observed at the high percentiles (Fig. 5).

-The resolution plays an important role and is associated with better representing the moist processes. This is consistent with previous studies highlighting the relevance of diabatic processes [4,5,6] for the blocking development.

-The final production runs are coming soon; stay tuned!

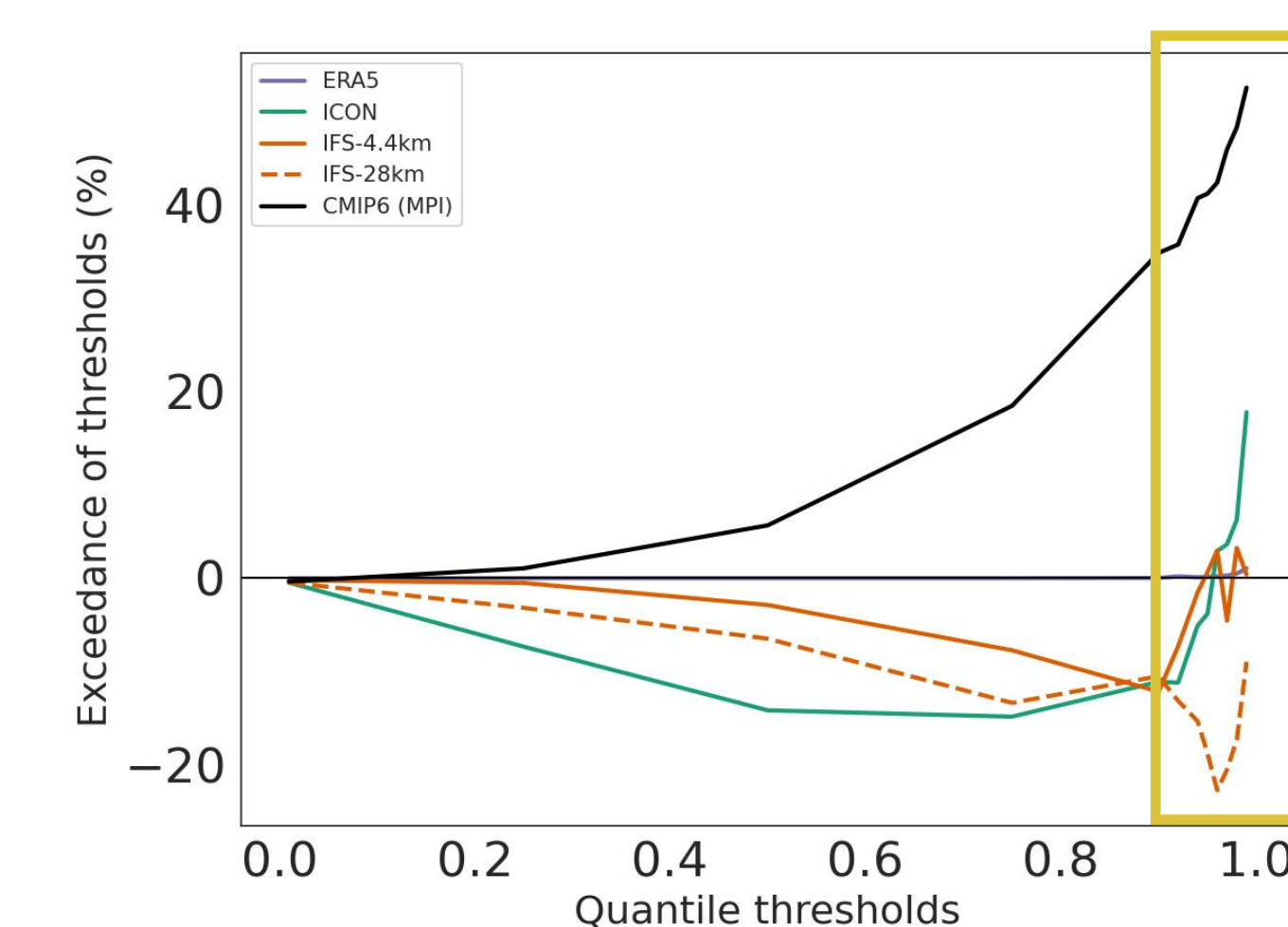


Figure 5. Events exceeding the ERA5 percentiles in the atmospheric blocking intensity of the **nextGEMS** and CMIP6 models

Reference:

[1] Dee et al., 2011
[2] Eyring, et al., 2016
[3] Schierz et al., 2004

[4] Maddona et al., 2014
[5] Pfahl et al., 2016
[6] Steinfeld et al., 2020

ConTrack

